Anisotropic magnetic site susceptibilities of the weak ferromagnet Au_4V above and below its Curie temperature

Anisotropic magnetic site susceptibilities of the weak ferromagnet Au_4V above and below its Curie temperature

P J Brown[1,2]**, A P Gandy**[2] **and K R A Ziebeck**[1]

[1] Institut Laue-Langevin, BP 156, 38042 Grenoble, France
[2] Department of Physics, Loughborough University, LE11 3TU, UK

Abstract
The distribution of magnetization aligned by a field of 9.8 T applied parallel to a general direction, close to [010], in Au_4V has been measured using polarized neutron diffraction. Measurements were made at 4 K, in the ferromagnetic phase, and in the paramagnetic phase at 80 K. The sample was only partially ordered and the results show that magnetic moments on vanadium atoms at both types of site in the structure are aligned by the field. At 4 K, 0.4 and 0.14 μ_B were aligned at the 2(a) and 8(h) sites respectively; these dropped to 0.1 and 0.03 μ_B at 80 K. The data can be modelled by assigning different anisotropic magnetic susceptibilities to vanadium atoms on the two sites. At 4 K, both sites show high anisotropy with a [001] easy axis, $\chi_\parallel/\chi_\perp \approx 5.5$ for the origin (2(a) V) site. The c-axis component of the moment of the V atoms on the 8(h) (Au) sites in the ferromagnetic phase is found to be oppositely aligned to that on the 2(a) sites, suggesting an antiferromagnetic exchange interaction. In the paramagnetic phase the anisotropy at the 2(a) sites is much smaller and there is no significant moment parallel to [001] on the 8(h) sites. The magnetization distribution around the 2(a) sites at 4 K contained significant non-spherical components. These suggest that the unpaired electrons are predominantly of t_{2g} character.

1. Introduction

Gold–vanadium alloys in the composition range 8–28 at.% V have been shown to undergo an order–disorder transition at 565 °C from a disordered fcc structure to one of the Ni_4Mo (D1a) type with space group $I4/m$ [1]. When fully ordered, the V atoms occupy 2(a) sites $(0, 0, 0)$ and the Au atoms the 8(h) sites $(x, y, 0)$. The ordered structure is simply related to the disordered face centred cubic phase as shown in figure 1. The effect of ordering is to separate the vanadium atoms, so that in the completely ordered phase all twelve near neighbours of the vanadium atoms are gold atoms. The ordered phase of Au_4V has been shown to be ferromagnetic,
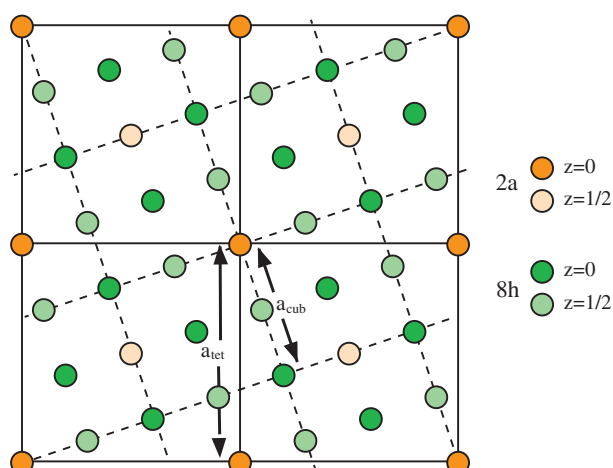
Figure 1. [100] projection of the ordered structure of Au_4V showing the relationship between the cubic and tetragonal cells which share a common *c*-axis.

T_C = 43 K, with a moment of ≈0.4 μ_B per V atom [2]. The magnetization shows a high degree of anisotropy with the easy axis parallel to [001]. Above the Curie temperature the uniform susceptibility follows a Curie–Weiss law with an effective paramagnetic moment of 1.49 μ_B per V atom. The magnetic properties of this alloy are unusually sensitive to the state of atomic order [3–5]. This behaviour and also the susceptibilities of more dilute Au–V alloys have been interpreted in terms of a model in which d-electron localization is inhibited by the presence of other vanadium atoms at distances of less than about 3.5 Å [3]. These authors point out that the V–V distance in the ordered alloy (3.98 Å) is too great for direct exchange to be significant and suggest that the exchange mechanism leading to ferromagnetism must involve the conduction band. Support for this interpretation is provided by self-consistent spin-polarized APW calculations of the band structure of metallic vanadium carried out as a function of lattice parameter. These calculations have established a critical V–V distance of about 3.2 Å below which the stable state of the vanadium atom is non-magnetic [6, 7].

An early investigation of the magnetization distribution in a partially ordered crystal of Au_4V showed that the ferromagnetic magnetization is essentially localized on the vanadium 2(a) sites [8]. Analysis of the departure from spherical symmetry of the magnetization distribution around the 2(a) site indicated a slight imbalance in the occupancies of the five symmetry adapted 3d orbitals. More than 20% of the magnetization was associated with $3z^2 - r^2$ orbitals and less than 20% with each of the $x^2 - y^2$ and xy orbitals. This corresponds to a magnetization distribution extended towards the near neighbour 2(a) sites in the [001] direction. These measurements were made with the field parallel to the [001] easy axis. Owing to the high anisotropy it was not possible to align a measurable moment perpendicular to [001] with the fields available at that time. In the present experiment we have used a 10 T superconducting magnet and a general crystal orientation to study the distribution of magnetization aligned in the hard as well as in the easy direction in both the ferromagnetic phase at 4 K and in the paramagnetic phase at 80 K.

2. Crystallographic structure and twinning

The crystal used in the present experiment was the same one as was studied previously [8]. Before the experiment it was examined using the neutron Laue technique which revealed that

it was by no means single. It was however possible to identify a single large grain of the tetragonal structure on which measurements could be made. The ordering process in Au$_4$V can give rise to six twin domains. These arise from three possible choices for the tetragonal c-axis: the three cubic $\langle 100 \rangle$ directions with, for each of these, two possible choices for the a-axis: cubic $[\frac{3}{2}\frac{1}{2}0]$ or $[\frac{3}{2}\frac{\bar{1}}{2}0]$. The fundamental reflections, those of the fcc lattice, are common to all twin components. For the chosen grain, superlattice reflections were found for only one of the six possible tetragonal orientations. The integrated intensities of 443 reflections from this grain with $\sin\theta/\lambda < 0.65$ Å^{-1} were measured on the four-circle diffractometer D15 at ILL using a neutron wavelength of 1.17 Å. The crystal was mounted in a two-stage Displex refrigerator and data were collected at 15 K and at 80 K. After correcting for absorption and averaging over equivalents, two data sets each containing 98 independent reflections were obtained. In the analysis of these data the possibility of the existence of differently oriented tetragonal twins was taken into account. For the tetragonal cell of the chosen grain the fundamental reflections have $3h + 5k = 3n$ with n integer and these reflections are common to all six twins. All the other reflections belong to just the chosen twin.

A least squares refinement of the structural parameters was carried out, using the measured integrated intensities as data, in which the possible contribution of each domain to the intensity was summed. The refinement allowed the relative populations of the six domains to be included as parameters. In the present case, the failure to observe superlattice reflection from five of the six domains suggests that their populations are small. Since these five domains only contribute to the fundamental reflections in the data sets and these reflections have nearly equal structure factors for all twins, their populations were constrained to be equal. As might be expected there was a strong correlation between the domain populations and the ordering parameter. However it was found that allowing the population of the major domain to drop below 85% led to unrealistically large values for the temperature factor of the 2(a) site. The best refinement was obtained with 92% of the crystal belonging to the major domain, and the results are given in table 1; they are in good agreement with those obtained in the previous study [8]. In the refinement of the 80 K data the domain populations, scale factor and site occupancies were fixed to the values obtained from the 15 K refinement. The position and thermal parameters obtained are included in table 1. There was no evidence for significant extinction in either set of data. As expected the contribution of the minority domains to the intensities is small and an almost equally good fit was obtained by fixing the majority domain population to unity. This assumption did not make any significant difference to any of the structure parameters.

3. Polarized neutron measurements

The same large grain from which the integrated intensity measurements were obtained was studied on the polarized neutron diffractometer D3 at the ILL. It was oriented with the direction $[1\bar{5}\bar{2}]$ approximately parallel to the field direction of a 10 T superconducting magnet and magnetized with a field of 9.8 T. The normal beam geometry of the diffractometer and the windows of the superconducting magnet allow access to reflections for which the inclination $90° - \nu$ of the scattered beam to the axis of the magnet lies in the range given by $-25° < \nu < 5°$. A preliminary measurement of the flipping ratios of all accessible reflections with $\sin\theta/\lambda < 0.5$ for which the absolute value of nuclear structure factor calculated from the structure parameters was greater than 4 fm was made using a rather short counting time. The measurements were then repeated with longer counting times, omitting all those reflections for which it was estimated that the standard deviation could not be reduced below ≈ 0.025 μ_B per V in the time available. The resulting list contained 40 independent reflections. The flipping ratios of these 40 reflections were remeasured in the paramagnetic phase at 80 K.

Table 1. Structure parameters refined for Au_4V.

Space group $I4/m$			$a = 6.361(5)$		$c = 4.009(3)$ Å at 15 K	
Majority domain population			94(5)%			

	Occupancy (%)						
Site	V	Au	T (K)	x	y	B (Å^2)	χ^2
2(a)	52(1)	48(1)	15	0	0	0.57(7)	2.6
			80	0	0	0.57(4)	2.5
8(h)	12.0(3)	88.0(3)	15	0.2018(1)	0.3986(1)	0.33(3)	
			80	0.2019(1)	0.3984(1)	0.50(1)	

Examination of the 4 K measurements revealed that there were very significant differences between the flipping ratios of equivalent reflections, even allowing for geometrical effects due to the different inclination of their scattering vectors to the field direction. These differences were greatest in the low angle reflections. The flipping ratios measured for the two accessible reflections of the form {101} were $R = 1.195(18)$ for 011 and $R = 0.820(8)$ for $\bar{1}01$. Since $R - 1$ has opposite signs for the two measurements the magnetic structure factors of these two *equivalent* reflections must also be of opposite sign. Tetragonal symmetry can be lost if strong anisotropy leads to non-parallelism between the induced magnetization and the applied field when the latter is not parallel to the fourfold axis [001]. However, if only the vanadium in the 2(a) sites, which are at the origin of the unit cell, contribute to the magnetization, anisotropy alone will not allow the magnetic interaction vectors of equivalent reflections to have opposite signs. The change of sign which is observed therefore implies that, when the field is not in the [001] direction, the vanadium in the 8(h) sites also contributes to the magnetization.

4. Data analysis

The calculation of the magnetization distribution induced by an applied field in a magnetically anisotropic crystal, and its refinement from flipping ratio measurements has been treated by Gukasov and Brown [9]. This same technique has been used to analyse the present results. In the analysis each reflection was treated independently and an average flipping ratio was only calculated when repeated measurements of the same reflection had been made. The measured flipping ratios were used as data in a least squares fit to a model of the magnetization distribution in the twinned crystal which associated independent anisotropic susceptibilities with the 2(a) and 8(h) sites. The 2(a) site has point group symmetry $4/m$ so the susceptibility is described by two independent coefficients χ_{11} and χ_{33}. For the 8(h) site which has only m symmetry there are four coefficients: χ_{11}, χ_{22}, χ_{33} and χ_{12}. These six susceptibility coefficients were the parameters of a least squares refinement in which the twin population and structural parameters were fixed to the values obtained from the integrated intensity measurements. The results are given in table 2. As expected from the magnetization measurements in the ordered phase there is a large anisotropy in the atomic susceptibilities at both sites at 4 K; $\chi_\parallel/\chi_\perp \approx 5.5$ at the 2(a) site and rather less, ≈ 2.4, at the 8(h) site. The anisotropy within the **a**–**b** plane at the 8(h) site is small. Rather unexpectedly, the moment induced parallel to the c-axis at the 8(h) sites is in the opposite direction to that on the 2(a) sites, and to the [001] component of applied field. At 80 K in the paramagnetic phase the anisotropy at the 2(a) sites is no longer significant. At the 8(h) sites no significant magnetization is induced parallel to [001]. The total moment per vanadium atom aligned by the field at the 8(h) sites is greater, at both temperatures, than that aligned at
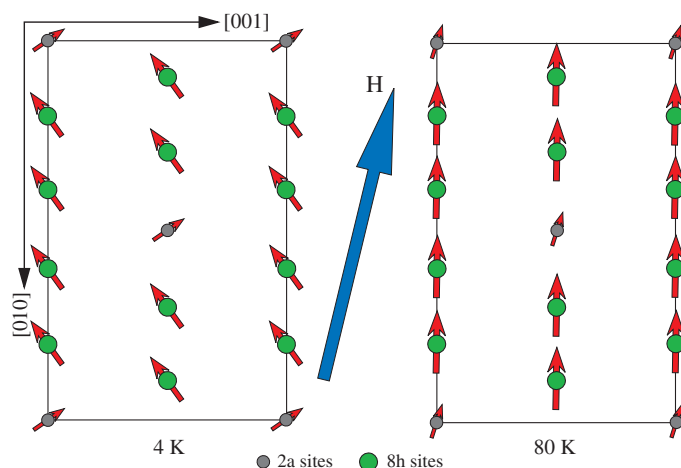
Figure 2. [100] projection of the unit cell of Au$_4$V showing the directions of the moments induced by a field parallel to the arrow labelled 'H', at 4 K and at 80 K. The lengths of the arrows are roughly proportional to the magnitudes of the moments induced per vanadium atom; the scale at 80 K is four times that at 4 K. Note that the vanadium occupancy of the 8(h) sites is only 12%.

Table 2. Susceptibilities and moments of vanadium atoms at the two sites of Au$_4$V in the ordered and paramagnetic phases.

| T (K) | Site | Susceptibility (10^{-1} μ_B T^{-1} V^{-1}) | | | | Moments (μ_B) | | χ^2 |
		χ_{11}	χ_{22}	χ_{33}	χ_{12}	Site[a]	per V[b]	
4	2(a)	0.453(7)		2.73(11)		0.401(7)	0.771(13)	6.5
	8(h)	1.09(2)	1.00(3)	−2.6(2)	−0.10(5)	0.138(4)	1.15(3)	
80	2(a)	0.184(3)		0.24(4)		0.097(2)	0.187(4)	1.1
	8(h)	0.317(11)	0.288(13)	0.01(7)	−0.03(2)	0.034(2)	0.281(12)	

[a] Moment aligned at the site calculated for 10 T.
[b] Aligned moment per vanadium atom calculated for 10 T.

the 2(a) sites. The magnitudes and directions of the moments aligned by the field at 4 K and at 80 K are shown schematically in figure 2.

In the previous experiment, the magnetization aligned by a field parallel to [001] was fitted by a moment centred on the 2(a) sites with a vanadium 3d form factor including a small negative orbital contribution amounting to some 4% of the spin moment and a small departure from spherical symmetry. The asphericity could be accounted for by preferential occupation by unpaired electrons, of the $3z^2 - r^2$, at the expense of the xy and $x^2 - y^2$ orbitals. With the present data, allowing an orbital moment did not significantly improve the fit, and the orbital parameter was found to be strongly correlated with the susceptibilities. A model in which the form factor associated with vanadium atoms on the 2(a) sites was expressed in terms of symmetry adapted multipoles up to order 4 gave a small improvement in the goodness of fit to the 4 K data without introducing strong correlation between parameters.

Under the point group symmetry of the 2(a) sites ($4/m$), the cubic degeneracies of the e$_g$ and t$_{2g}$ orbitals are lifted. The e$_g$ orbitals split into one of A$_g$ and one of B$_g$ symmetry: $3z^2 - r^2$, and $x^2 - y^2$ respectively. The t$_{2g}$ levels on the other hand split into a single state of B$_g$ symmetry: xy, and a doubly degenerate pair with E$_{1g}$ and E$_{2g}$ symmetries: xz and yz. The

Table 3. Multipole amplitudes determined for vanadium atoms at the 2(a) site in Au_4V at 4 K.

	Crystallographic axes	x rotated by 29° about [001]
χ_{11} (μ_B T^{-1})		0.0460(7)
χ_{33} (μ_B T^{-1})		0.279(11)
$Y(20)$	−0.007(4)	−0.007(4)
$Y(40)$	−0.293(13)	−0.293(13)
$Y(44+)$	0.043(13)	−0.093(11)
$Y(44-)$	−0.083(12)	−0.003(14)

Table 4. Matrix relating the multipole amplitudes to the occupancies of the different 3d orbitals. The final columns give the occupancies obtained from the experiment compared with those given in [8] for a *c*-axis field.

	Y(00)	Y(20)	Y(40)	Y(44+)	Occupancy (%)	
					a	b
$\|3z^2 - r^2\|^2$	1	$2\sqrt{5}/7$	6/7	0	2.1(8)	25
$\|x^2 - y^2\|^2$	1	$-2\sqrt{(5)}/7$	1/7	$\sqrt{5/7}$	11.9(8)	18
$\|xy\|^2$	1	$-2\sqrt{5}/7$	1/7	$-\sqrt{5/7}$	22.9(8)	16
$\|xz\|^2 + \|yz\|^2$	2	$2\sqrt{5}/7$	−8/7	0	63.1(11)	42

[a] Occupancies obtained for the multipole amplitudes of table 3.
[b] Occupancies with the applied field parallel to [001] [8].

two states with B_g symmetry can mix, and if the mixed states are given by

$$\psi_1 = \psi_{Bg1} \cos\alpha + \psi_{Bg2} \sin\alpha$$
$$\psi_2 = \psi_{Bg1} \sin\alpha - \psi_{Bg2} \cos\alpha \tag{1}$$

then the mixing can be eliminated by rotating the axes on which the states are described by an angle α about z. The magnetization distribution arising from unpaired electrons in these orbitals may be written as

$$M(\mathbf{r}) = \sum_{l,m} \rho(r) Y_l^m(\hat{\mathbf{r}}) \tag{2}$$

where the $Y_l^m(\hat{\mathbf{r}})$ are the spherical harmonic functions in the symmetry adapted combinations:

$$Y(00) = Y_0^0, \qquad Y(20) = Y_2^0, \qquad Y(40) = Y_4^0$$
$$Y(44+) = (Y_4^4 + Y_4^{-4})/\sqrt{2} \qquad Y(44-) = \iota(Y_4^{-4} - Y_4^4)/\sqrt{2}. \tag{3}$$

The coefficients of the five functions of equation (3) obtained from the least squares refinement are given in table 3. The combination $Y(44-)$ occurs due to mixing between the $x^2 - y^2$ and xy states. This is allowed because the orientation of the x-and y-axes in the (001) plane is not fixed by the 2(a) site symmetry. The relative magnitudes of the $Y(44+)$ and $Y(44-)$ coefficients depend on this orientation. It was found that rotation of the x-and y-axes by 29° about z, which puts the axes nearly parallel to those of the underlying cubic cell (figure 1), reduced the amplitude of $Y(44-)$ to zero. This implies that for this choice of axes the functions $x^2 - y^2$ and xy are independent. The matrix relating the occupancies of the four independent 3d orbitals to the amplitudes of the symmetrized functions, together with the occupancies deduced from the multipole parameters for this choice of axes, is given in table 4. The occupancies obtained by [8] with the field parallel to [001] are given for comparison in the final column of the table.

5. Discussion

The total moment aligned on the 2(a) sites in the ferromagnetic phase at 4 K by a field of 10 T parallel to [1$\bar{5}\bar{2}$] is 0.77(1) μ_B/V. This is only slightly greater than its component 0.6 μ_B/V along [001] and is compatible with the model of uniaxial anisotropy used by [5] to interpret the magnetization curves. The appearance of a moment associated with vanadium on the 8(h) sites is qualitatively at variance with the previous measurements; its anisotropy is much smaller than that found for the 2(a) sites, but even so the uniaxial anisotropy model would suggest that a moment of about 0.1 μ_B should have be found on the 8(h) sites in the previous experiment with an [001] field. The [001] component of the 8(h) site moment is in the opposite direction to the [001] component of applied field, suggesting antiferromagnetic coupling between the [001] components of the moment on the 2(a) and 8(h) sites. These observations imply that either the moment at the 8(h) sites is induced by the components of field applied in the (001) plane, or that the exchange coupling between the 2(a) and 8(h) sites is highly anisotropic and depends strongly on the components of moment in the (001) plane.

In the paramagnetic phase at 80 K the anisotropy of the site susceptibilities is much less and the aligned moments are nearly parallel to the applied field. There is no significant component of moment parallel to [001] at the 8(h) sites, suggesting some residual antiferromagnetic coupling. The ratio between the vanadium moments at the two sites is hardly changed.

The sizes of the moments induced at the 8(h) sites, and at both sites in the paramagnetic phase, are too small to allow the symmetries of the unpaired electrons which contribute to their magnetization to be determined. Comparison of the occupancies of the different 3d orbitals on the 2(a) sites at 4 K for the two field directions shows that the magnetization distribution at these sites depends on its orientation. Rotating the moment away from the [001] direction leads to a transfer of unpaired electrons at the 2(a) sites from the $3z^2 - r^2$ to the xz and yz orbitals. Naively such transfer could arise from a term in the Hamiltonian proportional to the x and y components of orbital momentum which would mix the xz and yz functions with z projection of orbital angular momentum $m = \pm 1$ into the $3z^2 - r^2$ function with $m = 0$. However this cannot provide a complete explanation since the results show that the orbital contribution to the magnetization is small. It does however seem likely that this orbital transfer is closely linked to the very strong magnetic anisotropy of vanadium at the 2(a) sites.

Au$_4$V has been classed with the weak itinerant ferromagnetic alloys ZrZn$_2$ and ScIn$_3$ which contain only atoms which do not normally exhibit ordered magnetism. In ZrZn$_2$ as in Au$_4$V the magnetization does not saturate even in rather high applied fields [11]. However the explanations given for this effect are completely different; in ZrZn$_2$ the lack of saturation is ascribed to the presence of low energy magnetic excitations characteristic of a weak ferromagnet, whereas in Au$_4$V any increase in magnetization due to magnetic excitations is obscured by much larger effects due to magnetic anisotropy. In ZrZn$_2$ the magnetic anisotropy is small; 0.05 T is sufficient to align all moments in the applied field direction [12], and the magnetization is largely delocalized through the overlap of the Zr 4d electron wavefunctions [10, 11]. In Au$_4$V on the other hand the anisotropy is strong and the magnetization is localized on the vanadium atoms. In this respect Au$_4$V is more like UGe$_2$ which also exhibits both weak ferromagnetism and high magnetocrystalline anisotropy and in which the U 5f electrons are supposed to exhibit 3d-like properties [13]. It is widely accepted that it is spin fluctuations which drive the Curie transition in weak itinerant ferromagnets [14]. Such spin fluctuations also dominate the paramagnetic response leading to the large effective moments characteristic of these systems. In this picture the local moments do not collapse at T_C, a prediction supported by polarized neutron diffraction measurements on Ni [15] and ZrZn$_2$ [10] which show that the spatial distribution of magnetization, and hence the states

occupied by the magnetic carriers, are unchanged in the passage into the paramagnetic phase. In Au_4V a multipole analysis of the magnetization distribution above T_C was not possible, but, since the ratios of the moments at the 2(a) and 8(h) sites are the same in the ferromagnetic and paramagnetic states, there can be no fundamental redistribution of magnetic carriers.

The observation that there is a larger moment induced on each vanadium atom at an 8(h) site than on one at a 2(a) site is difficult to reconcile with the interpretation given by Moruzzi *et al* [6] for the sensitivity of the saturation magnetization to the degree of atomic order. In their model, d-electron localization is inhibited by the presence of V neighbours at distances of less than about 3.2 Å. In the present Au_4V alloy the probability that a V atom at an 8(h) site has at least one close V neighbour is 0.98 compared to 0.78 for a 2(a) site; the model would therefore suggest that the V atoms at the 2(a) sites should have the largest moments. The present results show that a 3d moment can be stabilized on all the sites of the structure. On the other hand, the degree to which moments at the 2(a) and 8(h) sites can be aligned depends strongly on the direction as well as the magnitude of the applied field.

Acknowledgments

References

[1] Köster W and Nordskog H 1960 *Z. Metallk.* **51** 501
[2] Creveling L, Luo H L and Knapp G S 1967 *Phys. Rev. Lett.* **18** 851
[3] Creveling L, Luo H L and Knapp G S 1968 *Phys. Rev.* **176** 614
[4] Chin G Y *et al* 1968 *Solid State Commun.* **6** 153
[5] Adachi K, Matsui M and Fukuda Y 1980 *J. Phys. Soc. Japan* **48** 62
[6] Moruzzi V L, Marcus P M and Patnaik P C 1988 *Phys. Rev.* B **37** 8003
[7] Kubler J 1984 *J. Magn. Magn. Mater.* **45** 415
[8] Brown P J and Ziebeck K R A 1976 *Proc. Conf. on Neutron Scattering (Gatlinberg, TN)* p 616 (ORNL CONF-760601-P2)
[9] Gukasov A and Brown P J 2002 *J. Phys.: Condens. Matter* **14** 8831
[10] Brown P J, Ziebeck K R A and Mattocks P G 1984 *J. Magn. Magn. Mater.* **42** 12
[11] van Deursen A P J *et al* 1986 *J. Magn. Magn. Mater.* **54** 1113
[12] Ogawa S J 1976 *J. Phys. Soc. Japan* **40** 1007
[13] Saxena S S *et al* 2000 *Nature* **406** 587
[14] Moriya T (ed) 1985 *Spin Fluctuations in Itinerant Electron Magnetism* (Berlin: Springer)
[15] Brown P J, Deportes J and Ziebeck K R A 1991 *J. Physique* I **1** 1529